Multi-dimensional Distribution Matching for Probabilistically Shaped High Order Modulation Format

Mengfan Fu, Qiaoya Liu, Xiaobo Zeng, Yiwen Wu, Lilin Yi, Weisheng Hu, and Qunbi Zhuge*
State Key Laboratory of Advanced Optical Communication Systems and Networks, Department of Electronic Engineering, Shanghai Jiao Tong University, Shanghai, 200240, China
**Corresponding author: qunbi.zhuge@sjtu.edu.cn*

Abstract: We propose a multi-dimensional distribution matcher for probabilistically shaped high order modulation format. Compared to product distribution matching, 0.3 dB and 0.1 dB gains are obtained with the same complexity and 50% lower complexity, respectively.
OCIS codes: (060.2330) Fiber optics communications, (060.4080) Modulation

1. Introduction

To further increase optical communication capacity, probabilistic shaping (PS) for high order modulation format has attracted increasing attentions [1, 2]. One essential building block to implement the PS is distribution matching (DM). Many DM schemes have been proposed such as constant composition distribution matching (CCDM) [3], multiset partition distribution matching (MPDM) [4], enumerative sphere shaping (ESS) [5], and so forth. However, the complexity of these DM schemes is still an issue for efficient hardware implementation especially for high order modulation formats. Product distribution matching (PDM) [6] and parallel-amplitude distribution matching (PADM) [7] have been proposed to reduce the shaping complexity and latency of high order formats by using multiple parallel bit-level DMs instead of one symbol-level DM. Compared with PADM, PDM has a better performance for short block lengths. However, a gap still exists between the probability distribution of PDM and the Maxwell-Boltzmann (MB) distribution, which is the optimal probability distribution in the linear channel.

In this paper, we propose a multi-dimensional distribution matching (MDDM) scheme based on the bit-level DM architecture. In this scheme, the PS is implemented on higher dimensional symbols without increasing the complexity, and a novel mapping method is proposed to achieve an optimal probability distribution. By simulations, we show the proposed MDDM over 2 dimensions achieves 1.2 dB and 0.3 dB gains compared with CCDM and PDM, respectively. Furthermore, we show that one or more bit-level DMs can be omitted for complexity reduction, and it still achieves 0.1 dB gain with 50% lower complexity relative to PDM. Finally, the shaping gains are validated in experiments.

2. Multi-dimensional Distribution Matching

In a traditional PS architecture [8], as shown in Fig. 1 (a), one shaped quadrature amplitude modulation (QAM) symbol, regarded as a two-dimensional (2D) symbol, can be produced by two independently shaped amplitude shift keying (ASK) symbols. Alternatively, the PS can be implemented directly on 2D QAM symbols as illustrated in Fig. 1 (b). In general, the PS on 1D symbols has a lower complexity and almost the same performance as that on 2D symbols. The CCDM and PDM were both proposed for implementing the PS on 1D-symbols. Compared to the CCDM, the PDM shows a lower complexity and a better performance for short blocks. The implementation of the PDM is based on a bit-level DM architecture, which is shown in Fig. 1 (c). Since each amplitude can be represented by multiple bits, the probability of each amplitude can be obtained based on the product of the corresponding probabilities of the bits. Therefore, a symbol-level DM can be composed of multiple bit-level DMs. In the PDM, a gap exists between the resulted probability distribution and the optimal probability distribution, leading to a performance loss.

We propose a DM scheme to implement the PS on 2D-symbols based on the parallel bit-level DM architecture, as shown in Fig. 1 (d). Comparing Fig. 1 (d) with Fig. 1 (c), the numbers of required bit-level DMs for PDM (1D) and the 2D-DM are the same, so they have the same complexity. In the 2D-DM, the input bit length allocation of each bit-level DM can be optimized over more dimensions so that the probability distribution can be closer to the MB distribution. Therefore, the 2D-DM can achieve a better performance compared to PDM. Note that the same scheme can be extended to higher dimensions, which might further improve performance.

As illustrated in Fig. 1 (d), the implementation of the 2D-DM can be divided to two stages. First, the input $2k$ bits are allocated to the m bit-level DMs and each DM outputs n bits, where n is the block length. Second, the m parallel output bits are mapped to a 2D-symbol as the output of the 2D-DM. The symbol probability distribution of the 2D-DM depends on not only the binary probability distribution of each bit-level DM, but also the mapping function of each symbol. In the PDM, a natural based binary code (NBBC) is used to implement the mapping. Nonetheless, since NBBC cannot get a decreasing probability distribution on the powers of multi-dimensional symbols, it is not a good choice for the MDDM. We propose to use a look-up table (LUT) to implement the mapping. In particular, the binary probability distribution of each bit-level DM and the LUT are jointly optimized to achieve the optimal performance.

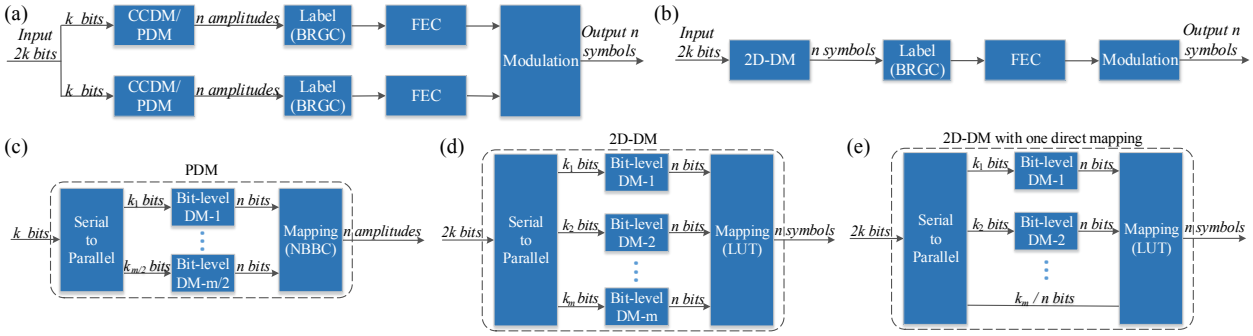

Fig. 1. (a) The transmitter architecture of PS; (b) The transmitter architecture of two-dimensional probabilistic shaping; (c) The schematic of PDM; (d) The schematic of 2D-DM; (e) The schematic of 2D-DM with one direct mapping.

It is known that in the PS the average transmit power should be minimized for a better performance, so we need to optimize both the binary probability distribution of each bit-level DM and the LUT to achieve the lowest power. For each input bit sequence allocation, there exists a corresponding binary probability distribution of each bit-level DM and we can get the probability distribution of each m-bit combination. The LUT implements a mapping that, the output QAM symbols with power in an ascending order are mapped to the binary codes with a probability in a descending order. In this way, the minimum average transmit power under the binary probability distributions can be obtained. By going through all possible input bit sequence allocation cases, we can obtain the configuration with the lowest power. This optimization process can be conducted offline without inducing extra complexity.

To reduce the complexity, some bit-level DMs in Fig. 1 (d) can be replaced by direct mapping, which means the output bit sequence is the same as the input bit sequence. The 2D-DM with one direct mapping is shown in Fig. 1 (e). The input length of the other bit-level DMs and the LUT should be re-optimized to minimize the performance loss.

3. Numerical and experimental Results

We first numerically evaluate the performance of 256QAM shaped via the 2D-DM in additive white Gaussian noise channels. For comparison, the results of the CCDM and PDM are included. Binary CCDM was used as the bit-level DM in both the 2D-DM and PDM. We chose 80 and 120 as the block lengths. For the same constellation and spectral efficiency (SE), the performance can be evaluated by the average transmit power. We took CCDM as a baseline for comparison and calculated the theoretical gain via $10\times log_{10} P_{CCDM}/P_{PDM/2D-DM}$. In addition, normalized generalized mutual information (NGMI) with a threshold of 0.78 was used for performance evaluation [9, 10].

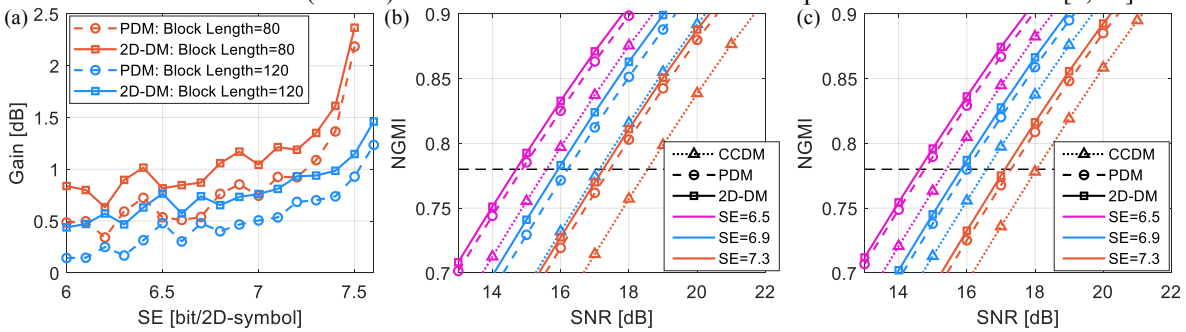

Fig. 2. Performance comparison of 2D-DM, PDM and CCDM: (a) Theoretical gain relative to CCDM; (b) NGMI for the block length of 80; (c) NGMI for the block length of 120.

Fig. 2 (a) shows the theoretical gain relative to the CCDM with the same block length as a function of SE. The fluctuation of the curves is caused by the different rate losses of the CCDM at different SEs when the block length is short. The 2D-DM provides more than 0.8 dB and 0.5 dB gains when the SE is larger than 6.3 bit/symbol for 80 and 120 block lengths, respectively. The gain increases as the block length decreases because the performance of the CCDM degrades sharply due to the quantization induced rate loss. On the contrary, the 2D-DM and PDM can reduce the rate loss by optimizing the bit-level DMs. Compared to the PDM, the 2D-DM achieves about 0.3 dB gain in average for both block lengths. Fig. 2 (b) and (c) show the NGMI as a function of signal-to-noise ratio (SNR) for 80 and 120 block lengths, respectively. At 6.9 bit/symbol SE, compared to the CCDM and PDM, for the block length of 80, the 2D-DM achieves 1.2 and 0.3 dB gains, respectively and for the block length of 120, 2D-DM achieves 0.75 and 0.18 dB gains, respectively. Both results are consistent with the theoretical gains in Fig. 2 (a).

The performance of the reduced-complexity 2D-DM is also evaluated and compared with the PDM. Since one 256QAM symbol contains 6 amplitude bits, there are at most 6 bit-level DMs. The numbers of bit-level DMs for the 2D-DM can be from 1 to 6. For the PDM, since one 16ASK symbol contains 3 amplitude bits, there are at most 3 bit-

level DMs. And the numbers of bit-level DMs for the PDM are 2, 4, and 6.

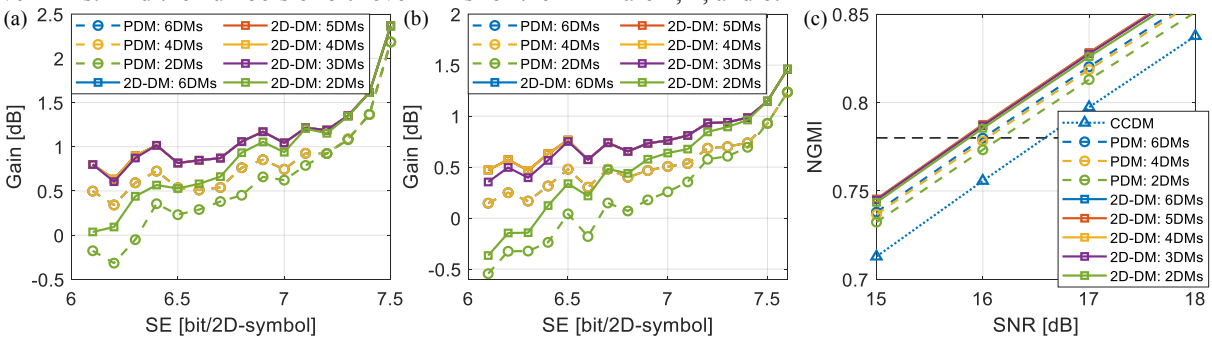

Fig. 3. Performance evaluation of reduced-complexity 2D-DM and PDM: (a) Theoretical gain relative to CCDM for block length of 80; (b) Theoretical gain relative to CCDM for block length of 120; (c) NGMI for block length of 120 at a SE of 6.9 bit/symbol.

Fig. 3 (a) and (b) show the theoretical gain of the 2D-DM and PDM with different DM numbers relative to CCDM. The PDM with 4 and 6 bit-level DMs have the same gain, because their optimized input bit allocations of each bit-level DMs are the same. For the 2D-DM, 4 to 6 bit-level DMs achieve identical gains. These curves completely overlap in the figures. When the SE is over 6.5 and 6.7 bit/symbol for block length of 80 and 120, respectively, the 2D-DM with 2 bit-level DMs has better performance than the PDM with 4 bit-level DMs. In this case, the 2D-DM can reduce the complexity by 50% relative to the PDM. Fig. 3 (c) shows the results for a block length of 120 when SE is 6.9 bit/symbol. It is shown the 2D-DMs with 2 to 6 bit-level DMs have almost the same performance. The 2D-DM with 2 bit-level DMs provides 0.3 and 0.1 dB gains compared to PDM with 2 and 4 bit-level DMs, respectively.

The performance of the 2D-DM is also evaluated in experiments. The experimental setup is shown in Fig. 4 (a). At the transmitter, the shaped symbols passed through a root-raised-cosine (RRC) filter in the offline DSP. The output digital signals were converted into four analogue signals by an arbitrary waveform generator (AWG) with a sampling rate of 80 GSa/s and then each signal was driven by a radio frequency (RF) driver. Next the signals were modulated by a dual-polarization I/Q modulator (DP-I/Q mod). A tunable laser with a linewidth of 25 kHz was adopted. The output optical signal was amplified by an Erbium-doped fiber amplifier (EDFA). After 10km transmission of standard single mode fiber (SSMF), the received optical power (ROP) was controlled by a variable optical attenuator (VOA). After coherent detection, the electrical signals were sampled by a 100 GSa/s digital storage oscilloscope (DSO). The digital signals were processed offline and the DSP algorithms in the receiver were shown in Fig. 4 (a).

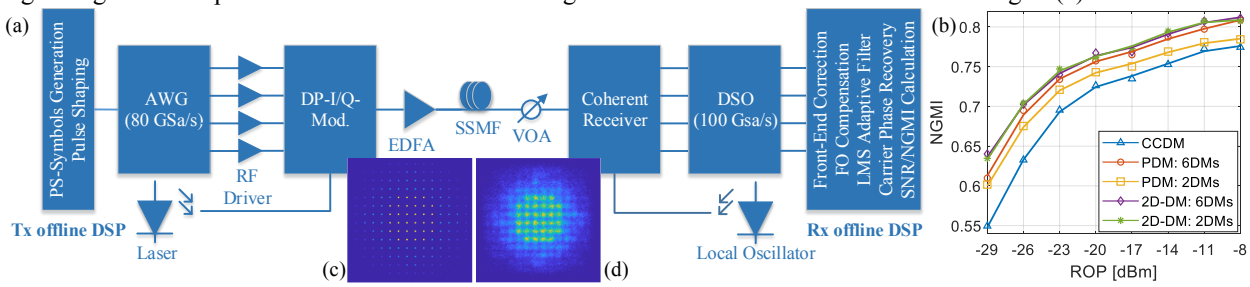

Fig. 4. (a) Experimental setup (FO: frequency offset); (b) Experimental result; (c) Transmitted constellation; (d) Received constellation.

The experimental results are shown in Fig. 4 (b). The transmitted and received constellations are shown in Fig. 4 (c) and (d), respectively. The SE is 6.9 bit/symbol and the block length is 120. The 2D-DMs with 2 bit-level DMs and 6 bit-level DMs have almost the same performance, and they outperform the CCDM and PDM with 2 bit-level DMs by the NGMI of 0.04 and 0.02, respectively, which is consistent with the simulation result in Fig. 3 (c).

4. Conclusions

In this paper, we proposed a 2D-DM scheme for shaped high order modulation format. Compared to the PDM, 0.3 dB and 0.1 dB gains are achieved with the same complexity and 50% lower complexity, respectively. The shaping gain is demonstrated in both simulations and experiments.

This work was supported by NSFC (61801291), Shanghai Rising-Star Program (19QA1404600) and National Key R&D Program of China (2018YFB1801203).

5. References

[1] M. Nakamura et al., in Proc. ECOC, Th1D, 2018.
[2] M. P. Yankovn et al., J. Lightw. Technol. 34(22), 5146 (2016).
[3] P. Schulte et al., IEEE Trans. Inf. Theory, 62(1), 430 (2016).
[4] T. Fehenberger et al., IEEE Trans. Commun., 67(3), 1885 (2019).
[5] Y. C. Gültekin et al., arXiv:1903.10244, Mar. 2019.
[6] G. Böcherer et al., arXiv:1702.07510, Feb. 2017.
[7] T. Fehenberger et al., arXiv:1902.08556, Feb. 2019.
[8] G. Böcherer et al., IEEE Trans. Commun., 63(12), 4651 (2015).
[9] J. Cho et al., in Proc. ECOC, M. 2. D., 2017.
[10] A. Alvarado et al., J. Lightw. Technol., 33(20), 4338 (2015)